



Mantle xenolith-bearing Maastrichtian to Tertiary alkaline magmatism in Oman

E. Gnos and T. Peters

Institut für Geologie, Universität Bern, Baltzerstrasse 1, 3012 Bern, Switzerland (gnos@geo.unibe.ch; tjerck@bluewin.ch)

[1] Mantle xenolith-bearing alkali basalts, basanites and tephrites with 1.5–2 K₂O and 4–5 wt% Na₂O occur as small (<100 m) plugs and dikes in the Batain and Haushi-Huqf areas, and WNW of Muscat. Their black color and the common presence of peridotite xenoliths allow a separation from older alkaline rocks and from the ophiolitic extrusive rocks. Two main dike directions, approximately E-W and N-S oriented, are observed. Intrusions seem to occur where these two fault systems intersect. The basalts crosscut the Upper Maastrichtian siliciclastic rocks of the Fayah Formation and the nappe stack of the Eastern Ophiolite Belt of the Batain area. They have not been observed intruding the Tertiary shallow marine carbonates although K-Ar whole rock dating on these lavas yielded Late Eocene 37 ± 1 to 44 ± 1 Ma ages. The rocks are aphyric and fine-grained with microgranular, and less common microtrachytic texture. They contain magmatic olivine (Fo_{80–82}), nepheline (Ne_{82–86}Ks_{14–18}), clinopyroxene (Di₄₆En₂₅Wo₂₈) with 2.5 wt% Al₂O₃, accessory phlogopite (X_{Mg}0.6, with 5.5 wt% TiO₂), in a microcrystalline or glassy matrix. Plagioclase is only observed in few samples. Locally occurring mm to cm-sized immiscible leucocratic melt droplets consist of potassium feldspar (An_{1–4}Ab_{37–39}Or_{60–70}), plagioclase (An_{20–22}Ab₆₅Or_{13–15}), nepheline (Ne₈₅Ks₁₅), phlogopite (X_{Mg}0.8, with ~6–7 wt% TiO₂), and titanomagnetite with ~8 wt% TiO₂. More than 95% of the xenoliths are <5cm-sized weakly to clearly foliated spinel peridotites of mantle origin. Sedimentary xenoliths (hornfels) are rare and lower crustal xenoliths were not found. The peridotite xenoliths consist of olivine (Fo_{90–92}), enstatite (En₈₉Fs₀₉Wo₀₂) with 3.1–3.3 wt% Al₂O₃, diopside (Di₄₅En₂₆Wo₂₉) with 3–6 wt% Al₂O₃, and Cr-spinel with ~60 mol% spinel, 20% hercynite, and 15–16% magnesiochromite. The age, chemical composition, and structural position suggest a relation with local tectonic movements associated with plate reorganization in the Owens Basin region prior to the Red Sea opening.

Components: 6840 words, 4 figures, 3 tables.

Keywords: Oman; chemistry; mineralogy; volcanic rocks; Indian Ocean; extensional tectonics.

Index Terms: 1099 Geochemistry: General or miscellaneous; 3040 Marine Geology and Geophysics: Plate tectonics (8150, 8155, 8157, 8158); 3625 Mineralogy and Petrology: Descriptive mineralogy; 9699 Information Related to Geologic Time: General or miscellaneous.

Received 17 October 2001; **Revised** 13 June 2002; **Accepted** 18 June 2003; **Published** 24 September 2003.

Gnos, E., and T. Peters, Mantle xenolith-bearing Maastrichtian to Tertiary alkaline magmatism in Oman, *Geochem. Geophys. Geosyst.*, 4(9), 8620, doi:10.1029/2001GC000229, 2003.

Theme: The Oman Ophiolite and Mid-Ocean Ridge Processes

Guest Editors: Peter Kelemen, Chris MacLeod, and Susumu Umino

1. Introduction

[2] Intracontinental alkaline volcanism occurs mainly in association with extensional tectonic regimes (e.g., Red Sea rifting) although transpressional tectonic settings are known [e.g., *Glazner and Bartley*, 1994]. In Oman alkaline volcanism in a continental setting occurred in association with the Permian-Triassic rifting and opening of the Neo-Tethys [e.g., *Glennie et al.*, 1974]. A contractional regime lasted from the Cenomanian to the end of Cretaceous resulting in thrusting of the Semail Ophiolite-Hawasina nappes complex in Campanian [e.g., *Glennie et al.*, 1974], and subsequently thrusting of the Eastern Ophiolite Belt (Batain nappes, Masirah ophiolites, Ras Madrekah and Ras Jibsch) at the Cretaceous-Tertiary boundary [e.g., *Gnos et al.*, 1997; *Peters et al.*, 2001]. Extension associated with reorganization of the plates after obduction of the Semail Ophiolite started at the end of the Maastrichtian [*Wyns et al.*, 1992a] thus coeval with the thrusting of the Eastern Ophiolite Belt. Associated tectonic movements gave way to eruption of alkaline olivine basalt (with olivine xenocrysts?) producing flows, pillowed lavas and volcanoclastic units. This late Maastrichtian volcanism is preserved in the terrestrial to marine Qahlah Formation [*Glennie et al.*, 1974; *Wyns et al.*, 1992b] of the Sur area.

[3] In the Haushi-Huqf area alkali basalts containing xenoliths derived from the Precambrian sedimentary strata and the underlying metamorphic and igneous Precambrian basement but not from the mantle were described by *Dubreuilh et al.* [1992a, 1992b]. These rocks, originally assumed to be Tertiary in age were subsequently recognized to be Ordovician in age [*Oterdoom et al.*, 1999]. However, the authors locate and describe in the same paper 20–30 km to the south other basalt intrusions which they interpret as Tertiary in age. WSW of Muscat, *Al-Harthy et al.* [1991] found alkali olivine basalts at Rusayl containing xenocrysts and small xenoliths of mantle origin. Mantle xenolith bearing alkali olivine basalts are also common in the Batain area [e.g., *Shackleton et al.*, 1990] located at the eastern end of the Oman Mountains (Figure 1). In this paper we will address

the mantle-xenolith bearing alkali olivine basalt outcrops of the Batain region in the southern Oman mountains (Figure 1) and compare them with the occurrence at Rusayl in the central Oman Mountains recognized by *Al-Harthy et al.* [1991].

2. Geologic Setting

[4] *Glennie et al.* [1974] recognized the allochthonous origin of the Batain sedimentary rocks and mapped them as Wahrah and Ibra Formations (Hawasina nappes) on their 1:500'000 scale map. *Shackleton et al.* [1990] published a more detailed map of the region describing several outcrops of black volcanic rocks as Tertiary, and referring to 37–44 Ma whole rock K-Ar ages obtained by A. C. Ries et al. (A continuation of geological studies in the Batain Coast Region, NE Oman, unpublished report, Amoco Petroleum Company, 1985). Geological maps, sheets Sur and Al Ashkharah at 1:250'000 scale, accompanied by explanatory notes were published by *Wyns et al.* [1992a, 1992b], *Béchenec et al.* [1992] and *Le Métour et al.* [1992]. On these maps additional localities of Tertiary volcanics are indicated. Only recently it was recognized that the Batain area to the east of the Jebel Ja'alan crystalline basement outcrops (Figure 1) is not part of the Semail Ophiolite-Hawasina nappe complex. The rocks of this area belong to a discontinuous Eastern Ophiolite Belt which was thrust onto the Arabian continent only at the Cretaceous/Tertiary boundary, thus 20 Ma after the Semail ophiolite obduction [*Gnos and Perrin*, 1995; *Gnos et al.*, 1997; *Schreurs and Immenhauser*, 1999; *Immenhauser et al.*, 2000]. These new ideas led to a detailed mapping of *Shackleton et al.*'s [1990] mélange [*Immenhauser et al.*, 1998; *Hauser*, 2000; *Moser*, 2000; *Peters et al.*, 2001], the recognition of a set of coherent sedimentary nappes forming the bulk of the Batain area, and a proper stratigraphic definition of the units present (Figure 1).

[5] *Filbrandt et al.* [1991] and *Wyns et al.* [1992a] discussed the Late Cretaceous to early Tertiary syn-sedimentary tectonic movements of the Jebel Ja'alan-Batain area. They recognized that detritus derived from the Hawasina nappes northwest and west of the Jebel Ja'alan formed alluvial fans

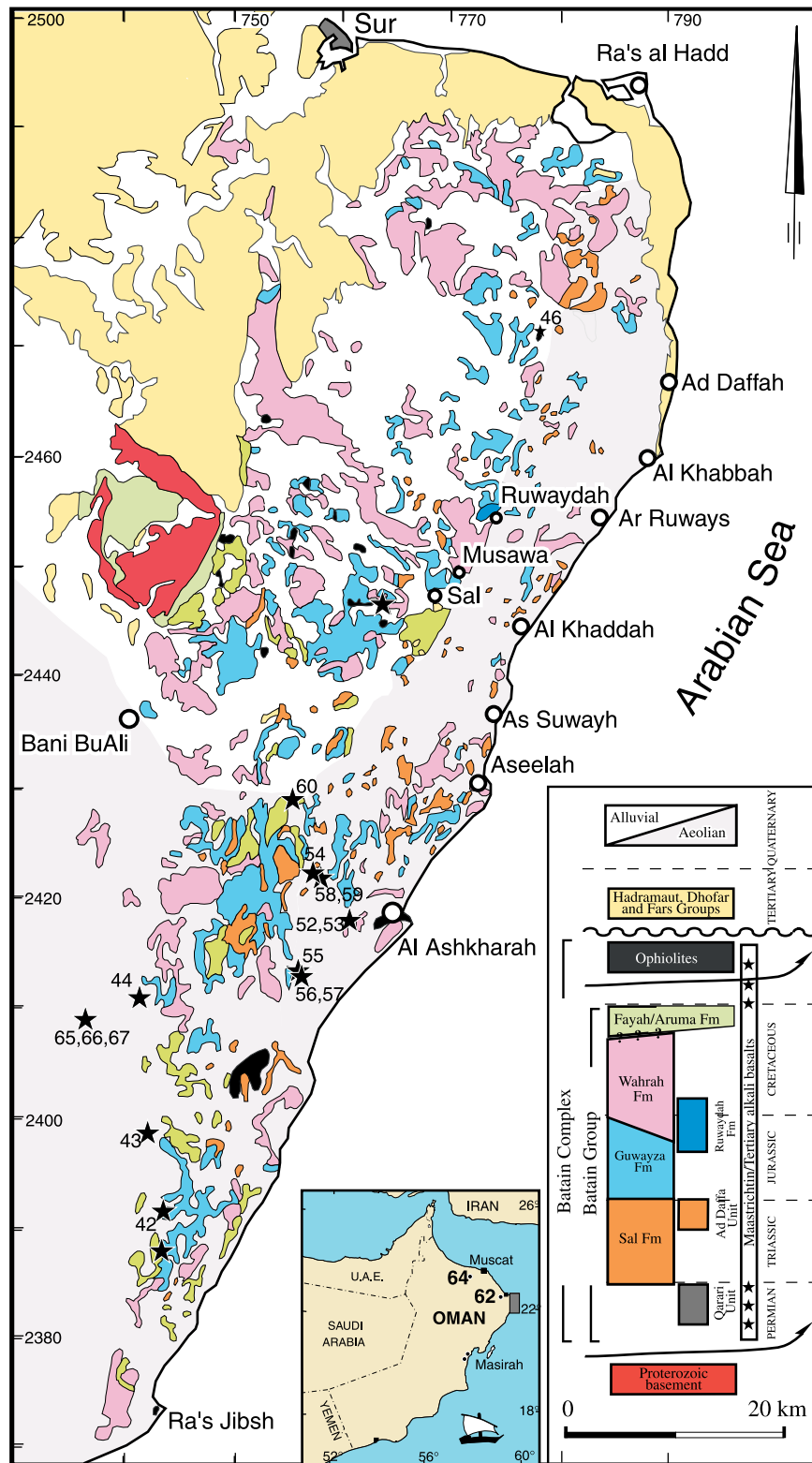


Figure 1. Geologic map of the Batain area, SE Oman, based on Hauser [2000]. Early Tertiary alkali basalt dikes and small intrusion [Le Métour et al., 1992; Peters et al., 2001, and own data] are marked with black stars. Numbers refer to localities discussed in the text.

during the end of Campanian to Maastrichtian [Filbrandt *et al.*, 1991]. Later in Maastrichtian the terrigenous input ceased and a shallow carbonate shelf established. Tectonic activity increased during the end-Maastrichtian/Paleocene causing reactivation of faults and uplift of the Jebel Ja'alan [Filbrandt *et al.*, 1991; Würsten *et al.*, 1991]. The main fault sets created or reactivated are oriented N-S to NNE-SSW (parallel to the trend of the Haushi-Huqf -Jebel Ja'alan horst) and E-W to ENE-WSW (for example northern edge of Jebel Ja'alan). The alkali basalt magma hence forms east or north trending dikes. Small plugs and intrusions seem to occur at intersections of the two faults sets. The intrusion may produce small thermal aureoles in the surrounding sedimentary rocks, as for example at Jebel Fayah. In the Batain area the intrusions crosscut sedimentary rocks of the Batain nappes [Peters *et al.*, 2001] and the Fayah Formation [Shackleton *et al.*, 1990] but were not observed in Eocene rocks. The same stratigraphic relationship was also recognised by Al-Harthy *et al.* [1991] in the central Oman Mountains where the basalts intrude the Paleocene Jafnayn Formation but not the Eocene strata. All known occurrences of such basalts in the Batain area are indicated in Figure 1 and additional sample localities are marked on the overview map.

3. Rock Description

[6] The alkali basalts form black dikes and plugs, sometimes with glassy appearance, and are easily recognized in the field. In most cases the lavas are aphyric containing only angular fragments of olivine xenocrysts and/or cm-sized mantle xenoliths. The basalts form small intrusions (Figure 2a) or dm to m-sized dikes (Figure 2b). Columnar jointing is locally observed at the contact to the wall rocks, and small thermal aureoles can be present. With few exceptions the dikes and intrusions contain 0.5–5 cm sized mantle xenoliths and xenocrysts, which can make up a few percents of the rock volume. Xenoliths from the Batain sedimentary nappes are also locally common and include red or green cherts, pale limestones and quartz-rich lithologies. Xenoliths of Precambrian sedimentary or crystalline basement rocks as

described from the Haushi-Huqf area to the south [Dubreuilh *et al.*, 1992a, 1992b] were not observed in the Batain region. Flows and pillow lavas were found at one locality (44; Figure 1) in the Batain region. Unlike the Mesozoic pillow lavas of the Batain thrust complex the pillow lavas belonging to the late Cretaceous/Tertiary magmatism are relatively fresh. They are ophitic to porphyritic (nepheline and pyroxene) in texture, locally amygdaloidal, and weather brownish. At Jebel Fayah white, mm to cm-sized droplets of a leucocratic magma can be observed in the dark basalt (Figure 2c). Similarly leucocratic cm-sized, irregular-shaped melt droplets occur also in the basalt intrusion at Rusayl. The isolated outcrop in the Wahiba Sands (Figures 1 and 2a) is especially rich in mantle xenoliths (Figure 2c). The basalt intrusion at Jebel Fayah (type locality of the Fayah Formation) [Shackleton *et al.*, 1990] is well accessible and shows most of the phenomena described above. For a description of the outcrops near the Sultan Qaboos University in the central Oman Mountains readers are referred to Al-Harthy *et al.* [1990].

[7] In thin section the basalts show porphyric microgranular texture (Figure 3a) containing euhedral olivine phenocrysts that are partly resorbed, subhedral to euhedral light brownish clinopyroxene (Figure 3a), nepheline laths (Figure 3b), locally plagioclase, and squares of titanomagnetite. Only at Rusayl (64) some clinopyroxene rims show the anomalous colors under crossed polarizers characteristic of Ti-augite. The groundmass consists of nepheline, potassium and calcic feldspar, clinopyroxene, glass (mainly devitrified), and locally abundant phlogopite (Figure 3c). Clinopyroxene may be slightly zoned and commonly contains small inclusions in the rim regions. Phlogopite shows dark rims, probably caused by formation of oxides due to oxidation. The nepheline crystals may display a strong alignment producing a microtrachytic texture. The leucocratic phonolitic melt droplets found at Jebel Fayah (Figure 2c) and Rusayl consist of potassium feldspar, nepheline, plagioclase, phlogopite and Ti-magnetite (Figure 3c). The xenoliths are medium-grained with equigranular textures (Figure 3d), and display weak to clear foliation. All xenoliths investigated are spinel-bearing and have

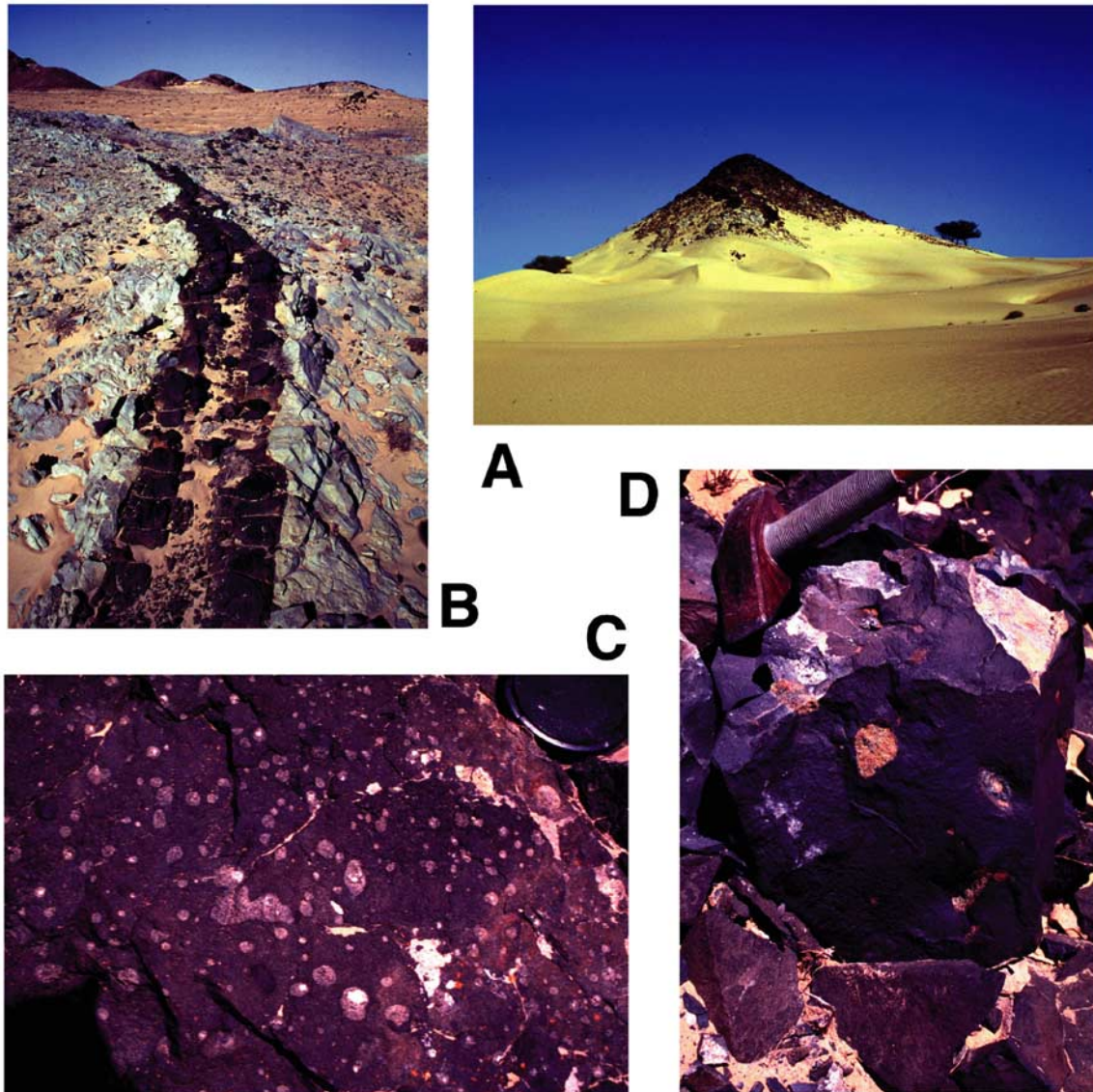


Figure 2. (a) Olivine basalt intruding Batain Group sedimentary rocks. Isolated outcrop in Wahiba Sands WSW of Al Ashkharah (locality 65–67). (b) E-W oriented Tertiary olivine basalt dike (width 0.5 m) intruding Triassic to Jurassic Matbat limestones (Sal Formation) of the Batain Group southwest of Al Ashkharah (locality 52,53 in Figure 1). (c) Detail of a basaltic intrusion displaying immiscible melts at Jebel Fayah (locality 42). The dark parts consist of nepheline-bearing olivine basalt, whereas the light phonolitic magma consists of nepheline, phlogopite, sanidine and plagioclase. Base of image 15 cm. (d) Spinel lherzolite xenoliths in basalt. Base of image ca. 30 cm, same locality as Figure 2a.

lherzolitic or harzburgitic mineralogy. In thin section the spinels are brown transparent and the pyroxenes are without exsolution lamellae. The olivine may contain few, wide-standing dislocation walls.

[8] Many xenoliths show trails of melt inclusions (healed cracks). Locally melt infiltrating along grain boundaries causes incipient xenolith desintegration. Along such grain boundaries growth of

small magmatic olivine and clinopyroxene is observed, and relic glass is found. Whereas the Batain dikes and intrusion contain generally only small amounts of mainly devitrified glass, the original glass content in rocks from the Rusayl locality [*Al-Harthy et al.*, 1991] is much higher and may reach 20% (Figure 3d). Some samples from the later locality are clinopyroxene-rich with crystals reaching cm-size. A thin section of a 5 mm

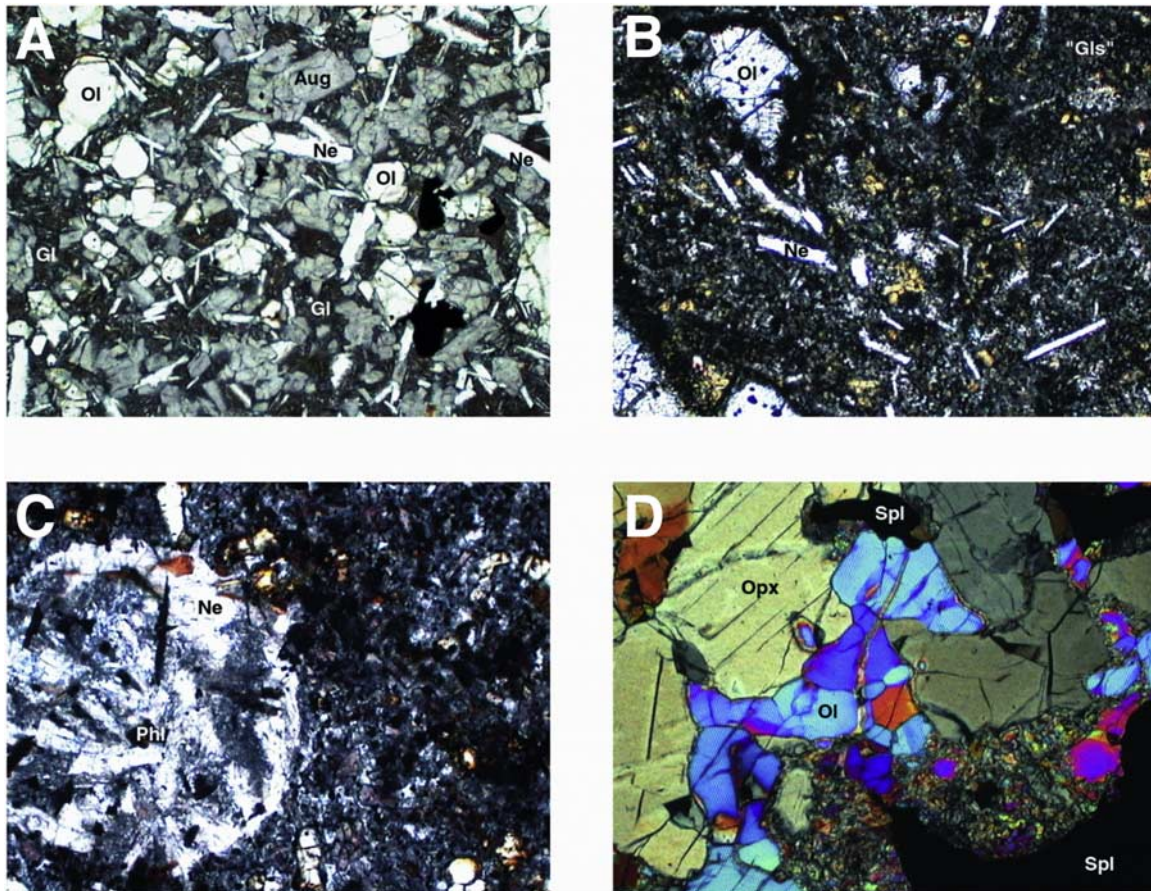


Figure 3. Thin section photographs of olivine basalt from the Batain region, base of images 3 mm. (a) Fine-grained rock (43B) containing olivine xenocrysts. Note the twin-free nepheline laths. The matrix (“Gl”) is mainly cryptocrystalline, containing small crystals of clinopyroxene and ?olivine. Plane polarized light. (b) Microphyric alkali olivine basalt (54) containing abundant clinopyroxene, olivine xeno- and neocrysts, nepheline laths, and Ti-magnetite. The amount of cryptocrystalline matrix (“Gls”) is <20% in this specimen. Plane polarized light. (c) Thin section photograph, plain polarized light, showing melt immiscibility (42A). The orbicular leucocratic magma patches consist of nepheline, plagioclase, sanidine and phlogopite, with minor aluminous diopside. The surrounding olivine-basaltic melt consists of olivine, augite, minor phlogopite, opaques, and cryptocrystalline matrix. Plane polarized light. (d) Spinel-bearing harzburgite xenolith (67B) showing basalt infiltration along grain boundaries. The melt-xenolith interaction zone is now represented by fine-grained material. Polarized nichols.

wide small contact aureole developed in Triassic silicified marly limestone (locality 59) contains 0.1–0.2 mm sized zoned grossularite garnets with a lemon core, colorless rim and anisotropic optical character. Associated with it occur optically anomalous zoisite, calcite, and wollastonite or scapolite.

4. Rock and Mineral Chemistry

4.1. Rock Chemistry

[9] Only rock material free of macroscopically visible xenocrysts was used. Major and trace

element concentrations were analyzed by XRF at the Fribourg/Bern facility. Fe^{2+} – Fe^{3+} concentrations were determined colorimetrically using the bipyridine method, and the H_2O content of the samples was analyzed with the Penfield method. Analyses are listed in Table 1. Most analyses fall in the basanite field with >10% normative olivine (Table 1; Figure 4) in the TAS diagram [LeMaitre *et al.*, 1989]. All rocks are nepheline normative (Table 1), and in many of the rocks nepheline is also recognizable in thin section. The two analyses from the Rusayl locality (OE64) show the lowest $\text{Na}_2\text{O} + \text{K}_2\text{O}$ contents, and the highest Ba, Sr and



Table 1. Whole Rock and Trace Element Data for Tertiary Alkali Basalts^a

	Jebel Fayah				Pillow Lava				Qalhah				Rusayl				Wahiba Sands				
	94OE 42B	94OE 42D	94OE 4A	94OE 43B	94OE 44A	94OE 44B	94OE 44C	94OE 44E	94OE 46	94OE 52	94OE 53	94OE 54	94OE 55	94OE 57	94OE 58	94OE 60	94OE 62	94OE 64B	94OE 64C	94OE 65	94OE 66
SiO ₂	43.07	42.72	44.78	44.31	48.38	47.69	46.14	44.49	42.70	43.30	46.19	43.41	45.91	42.69	44.08	45.55	40.31	39.87	41.55	41.81	
TiO ₂	2.19	2.04	2.21	2.22	3.20	3.27	3.27	2.25	2.17	2.16	2.26	2.35	1.84	1.98	2.10	3.69	1.51	1.40	2.05	2.04	
Al ₂ O ₃	13.44	13.51	13.93	13.93	13.64	13.95	17.66	14.10	13.34	13.32	14.99	13.86	13.88	12.32	13.55	14.63	12.57	12.41	13.07	12.88	
Fe ₂ O ₃	4.16	4.00	2.95	2.87	7.03	6.91	6.82	3.15	4.04	2.92	7.54	2.90	2.57	3.02	4.00	5.08	4.77	4.69	5.02	4.71	
FeO	6.64	6.29	7.72	7.82	5.41	5.91	3.71	7.51	6.40	7.48	2.74	7.93	7.66	6.79	6.38	7.73	3.72	3.38	6.43	6.67	
MnO	0.20	0.19	0.18	0.18	0.22	0.20	0.21	0.17	0.18	0.18	0.16	0.18	0.16	0.18	0.18	0.17	0.15	0.14	0.22	0.22	
MgO	11.04	11.14	10.58	10.44	3.79	3.82	3.96	10.25	11.33	11.64	7.94	11.23	9.99	13.92	11.65	6.83	16.04	12.09	9.83	10.15	
CaO	10.24	9.51	10.07	10.05	7.09	7.22	6.47	10.10	10.00	10.03	9.89	10.24	10.22	10.11	9.44	8.98	10.95	13.33	10.99	10.94	
Na ₂ O	4.99	4.53	3.96	3.97	5.20	4.58	4.50	4.12	3.44	4.20	4.12	3.74	3.82	3.87	4.67	2.71	1.41	2.23	5.05	5.16	
K ₂ O	1.81	2.15	1.91	1.82	1.57	1.96	1.66	1.74	1.93	1.66	2.00	2.12	1.66	2.23	1.17	1.73	1.14	1.52	2.31	2.36	
P ₂ O ₅	1.11	1.01	0.80	0.78	1.50	1.53	1.15	0.82	0.84	0.83	0.78	0.77	0.86	1.01	1.02	0.75	0.82	0.74	1.42	1.39	
H ₂ O ⁺	0.80	2.27	0.74	0.97	2.34	2.38	3.85	0.98	3.00	1.70	0.93	0.89	0.61	1.04	1.52	1.08	6.10	7.41	1.45	0.87	
CO ₂																					
Total	100.34	100.00	100.61	100.15	99.92	100.01	99.77	100.43	100.01	100.18	99.83	100.42	99.95	99.84	100.41	99.70	99.88	99.55	100.04	99.86	
Ba	813	1009	673	682	361	1023	688	716	828	784	543	709	801	805	612	1352	2293	2106	847	793	
Cr	320	313	277	275	8	11	23	215	313	315	219	213	217	459	333	73	317	282	240	251	
Cu	37	35	48	46	26	27	23	45	35	40	37	36	47	35	30	23	53	47	38	38	
Ga	19	17	18	19	30	28	25	18	18	18	17	19	17	15	14	26	14	12	18	15	
Nb	88	94	72	73	112	112	89	74	100	95	64	73	73	101	80	67	123	148	120	115	
Ni	236	246	186	184	bd	bd	8	179	268	259	112	205	168	371	318	62	416	424	160	168	
Pb	bd	bd	bd	bd	bd	bd	bd	bd	bd	bd	bd	bd	bd	bd	bd	bd	bd	bd	bd	bd	
Rb	29	48	45	48	9	19	31	22	44	32	39	29	33	50	16	21	29	39	64	53	
Sr	1085	1167	860	865	457	731	1930	889	876	918	839	909	982	982	946	1297	3150	3355	1417	1284	
Th	bd	bd	bd	bd	bd	bd	bd	bd	bd	bd	3	bd	bd	bd	bd	bd	6	8	bd	bd	
V	191	168	181	195	140	151	261	175	175	181	196	182	148	168	150	225	136	113	149	157	
Y	28	24	26	23	68	70	47	24	27	26	26	26	23	25	24	32	22	25	35	32	
Zn	88	81	86	88	157	160	112	84	87	85	77	85	72	73	82	116	69	73	92	91	
Zr	220	214	186	185	479	485	416	185	207	212	184	204	161	212	212	303	222	234	275	265	



Table 1. (continued)

	Jebel Fayah								Pillow Lava								Qalhhah								Rusayl				Wahiba Sands			
	94OE 42B	94OE 42D	94OE 4A	94OE 43B	94OE 44A	94OE 44B	94OE 44C	94OE 44E	94OE 46	94OE 52	94OE 53	94OE 54	94OE 55	94OE 57	94OE 58	94OE 60	94OE 62	94OE 64B	94OE 64C	94OE 65	94OE 66	94OE 65	94OE 66									
Or	8.96	11.9	11.43	10.97	9.64	12.03	10.34	10.46	10.46	11.89	10.08	12.08	11.27	9.99	3.26	7.07	10.50	6.79	0.00	0.00	0.00	0.00	0.00	0.00								
Ab	0.00	0.00	5.06	4.91	37.33	33.83	33.82	5.73	5.73	1.88	2.12	12.08	0.00	10.84	0.00	9.07	21.25	0.00	0.00	0.00	0.00	0.00	0.00	0.00								
An	9.07	10.54	14.78	15.11	9.60	12.17	24.34	15.09	15.91	12.93	16.87	16.87	15.02	16.11	9.88	12.84	23.27	26.49	21.01	6.34	5.13	6.34	5.13	5.13								
Lc	1.50	0.98	0.00	0.00	0.00	0.00	0.00	0.00	0.00	0.00	0.00	0.00	1.15	0.00	8.02	0.00	0.00	0.36	7.64	10.99	11.18	10.99	11.18									
Ne	23.24	21.49	15.64	15.90	4.53	3.48	3.43	16.10	15.42	18.63	12.76	17.43	11.95	11.95	18.15	16.98	1.25	6.96	11.09	23.77	24.19	23.77	24.19									
Wo	14.69	13.14	12.75	12.75	7.00	6.12	0.66	12.7	12.56	13.61	11.72	13.16	12.43	12.43	14.48	11.79	7.29	10.95	14.10	15.44	15.44	15.44	15.44									
En	8.85	8.04	7.60	7.56	2.59	2.23	0.28	7.51	7.72	8.41	6.58	7.98	7.30	7.30	9.51	7.30	3.60	7.65	9.10	8.73	8.89	8.73	8.89									
Fs	5.05	4.35	4.50	4.55	4.55	4.02	0.38	4.55	4.12	4.41	4.66	4.46	4.53	4.53	3.95	3.79	3.55	2.38	4.05	6.07	5.96	6.07	5.96									
Fo	13.38	14.49	13.39	13.29	5.06	5.36	7.09	12.94	15.21	14.98	9.56	14.34	12.64	12.64	18.2	15.68	9.73	24.79	16.53	11.5	11.89	16.53	11.89									
Fa	8.42	8.65	8.73	8.81	9.80	10.65	10.30	8.64	8.96	8.65	7.46	8.85	8.64	8.64	8.34	8.98	10.57	8.50	8.10	8.81	8.78	8.10	8.78									
Cs	0.00	0.00	0.00	0.00	0.00	0.00	0.00	0.00	0.00	0.00	0.00	0.00	0.00	0.00	0.00	0.00	0.00	0.00	3.64	0.97	1.2	3.64	0.97									
Il	4.23	4.01	4.25	4.30	6.31	6.45	6.55	4.35	4.30	4.21	4.39	4.54	3.56	3.56	3.85	4.08	7.20	3.09	2.89	4.00	3.96	2.89	4.00									
Ap	2.61	2.42	1.88	1.84	3.61	3.68	2.81	1.93	2.03	1.98	1.85	1.81	1.81	2.03	2.39	2.42	1.79	2.05	1.86	3.38	3.29	1.86	3.38									
Total	100.01	100.01	100.01	100.01	100.01	100.01	100.01	100.01	100.01	100.01	100.01	100.01	100.01	100.01	100.01	100.01	100.01	100.01	100.01	100.01	100.01	100.01	100.01									
Mg-No	65.16	66.46	64.28	63.91	36.19	35.67	41.33	63.62	66.53	67.00	59.43	65.29	63.90	63.90	72.04	67.28	49.44	77.86	71.6	61.2	62.06	71.6	62.06									
D.I.	33.70	34.37	32.14	31.79	51.50	49.33	47.59	32.29	29.20	30.82	36.92	29.85	29.85	32.78	29.42	33.12	33.01	14.11	18.74	34.76	35.37	18.74	35.37									
Pl-An	100	100	73.35	74.35	19.50	25.32	40.42	71.29	88.85	85.18	56.82	100.00	58.35	58.35	100.00	57.16	50.79	100.00	100	100	100	100	100									
Or	49.68	53.03	36.55	35.4	17.03	20.73	15.10	33.43	40.06	40.10	29.44	42.88	27.04	27.04	24.79	24.40	19.09	20.41	0.00	0.00	0.00	0.00	0.00									
Ab	0.00	0.00	16.19	15.85	66.00	58.3	49.36	18.32	6.34	8.44	29.45	0.00	29.34	0.00	0.00	31.30	38.62	0.00	0.00	0.00	0.00	0.00	0.00									
An	50.32	46.97	47.26	48.75	16.97	20.97	35.54	48.25	53.60	51.46	41.11	57.12	43.62	43.62	75.21	44.31	42.29	79.59	100.00	100.00	100.00	100.00	100.00									

^abd, below detection; Wo, En and Fs are normative pyroxene end-members, Fo, Fa and Cs (larnite) normative olivine end-members.



Table 2. Representative Magmatic and Xenolithic Mineral Compositions in Jebel Fayah Intrusion 42

	Mag			Mag Exs			Mag Exs			Xen			Mag			Xen			
	94OE 42A cpx3	94OE 42A sdn9	94OE 42A hmt1	94OE 42A cpx3	94OE 42A nph5	94OE 42A plg4	94OE 42A ph2	94OE 42A mgr7	94OE 42A ol6	94OE 42A sp17	94OE 42C plg24	94OE 42C spl1	94OE 42C ph11	94OE 42C cpx3	94OE 42C ol10	94OE 42C opx4	94OE 42C cpx23	94OE 42C spl22	
SiO ₂	47.15	63.35	0.08	64.83	46.98	49.72	61.46	34.82	0.02	41.06	0.02	54.53	0.02	35.79	52.03	40.40	56.28	51.30	0.05
Ti O ₂	2.54	0.08	13.53	0.03	2.33	0.00	0.08	5.46	7.31	0.02	7.31	21.80	6.42	0.94	0.00	0.09	0.85	0.60	0.60
Cr ₂ O ₃	0.01	0.00	2.72	0.00	0.00	0.04	0.05	0.02	21.34	0.00	21.34	1.03	0.05	0.43	0.00	0.17	0.19	6.75	6.75
Al ₂ O ₃	6.17	20.42	1.69	18.87	5.37	30.32	23.84	15.01	9.11	0.06	9.11	28.86	1.83	13.88	3.63	0.00	2.02	5.66	53.95
Fe ₂ O ₃ ^a	2.84	0.56	72.48	0.80	2.99	0.00	0.00	8.93	23.54	0.00	23.54	0.34	25.40	8.19	1.29	0.00	0.76	1.31	7.68
FeO	4.70	0.00	8.46	0.00	9.50	0.49	0.28	12.89	34.55	11.06	34.55	0.00	45.32	12.1	3.57	12.91	7.62	4.60	15.85
MnO	0.16	0.00	1.01	0.04	0.31	0.04	0.00	0.31	0.54	0.18	0.54	0.01	0.79	0.29	0.05	0.19	0.25	0.15	0.05
MgO	12.63	0.00	0.99	0.02	9.52	0.02	0.00	10.23	2.87	48.26	2.87	0.05	3.47	10.43	15.59	46.66	33.29	14.75	16.71
CaO	23.54	0.84	0.70	0.02	22.13	0.36	3.96	0.00	0.07	0.20	0.07	11.29	0.11	0.01	23.37	0.01	0.30	21.39	0.02
Na ₂ O	0.52	4.38	0.00	3.75	0.93	16.08	7.23	0.70	0.00	0.02	0.00	5.10	0.00	0.70	0.48	0.02	0.02	0.91	0.02
K ₂ O	0.00	10.33	0.03	12.49	0.01	2.85	2.59	9.19	0.00	0.00	0.00	0.48	0.00	9.26	0.01	0.00	0.01	0.00	0.01
H ₂ O ^a								4.02					4.02						
Total	100.27	99.96	101.69	100.76	99.97	99.92	99.49	101.57	99.35	100.87	99.35	100.77	99.77	101.17	101.41	100.20	100.82	101.13	101.68
Si	1.770	2.868	0.001	2.934	1.803	1.231	2.757	2.600	0.002	1.003	0.002	2.444	0.001	2.667	1.890	1.002	1.945	1.867	0.001
Ti	0.072	0.003	0.257	0.001	0.067	0.000	0.003	0.307	0.195	0.000	0.195	0.003	0.597	0.360	0.026	0.000	0.002	0.023	0.012
Cr	0.000	0.000	0.054	0.000	0.000	0.001	0.002	0.001	0.599	0.000	0.599	0.000	0.030	0.003	0.012	0.000	0.005	0.006	0.141
Al	0.273	1.090	0.050	1.003	0.244	0.885	1.261	1.321	0.381	0.002	0.381	1.524	0.079	1.219	0.155	0.000	0.082	0.243	1.681
Fe ³⁺	0.080	0.019	1.379	0.027	0.086	0.000	0.000	0.502	0.629	0.000	0.629	0.012	0.696	0.459	0.035	0.000	0.020	0.036	0.153
Fe ²⁺	0.148	0.000	0.179	0.000	0.305	0.010	0.010	0.805	1.025	0.226	1.025	0.000	1.381	0.754	0.109	0.268	0.220	0.140	0.350
Mn	0.005	0.000	0.022	0.002	0.010	0.001	0.000	0.019	0.016	0.004	0.016	0.000	0.024	0.019	0.002	0.004	0.007	0.005	0.001
Mg	0.707	0.000	0.037	0.002	0.546	0.001	0.000	1.139	0.152	1.758	0.152	0.004	0.189	1.159	0.844	1.725	1.715	0.800	0.659
Ca	0.947	0.041	0.019	0.001	0.912	0.010	0.190	0.000	0.003	0.005	0.003	0.542	0.004	0.001	0.910	0.000	0.011	0.834	0.001
Na	0.038	0.384	0.000	0.328	0.070	0.772	0.629	0.102	0.000	0.001	0.000	0.443	0.000	0.102	0.034	0.001	0.001	0.065	0.001
K	0.000	0.596	0.001	0.713	0.001	0.090	0.148	0.875	0.000	0.000	0.000	0.028	0.000	0.878	0.001	0.000	0.001	0.000	0.000
OH*							2.000						2.000						
X _{Mg} (Fe ²⁺)	0.827				0.641			0.586		0.880				0.606	0.886	0.864	0.886	0.851	
X _{Mg} (Fe ³⁺)	0.756				0.582			0.466		0.880				0.498	0.854		0.877	0.820	
Ab		0.376					0.650					0.438							
An		0.040					0.197					0.535							
Or		0.584					0.153					0.027							

^aCalculated value; mag, magmatic; xen, xenolithic; exs, leucocratic exsolutions.



Table 3. Representative Magmatic and Xenolithic Mineral Compositions in samples 64 (Rusayl) and 67 (Wahiba Sands)

	Mag				Xen				Mag				Xen			
	94OE 64C cpx1	94OE 64C sdn4	94OE 64C ne8	94OE 64C phl3	94OE 64C spl71	94OE 64C ol1	94OE 67A ol2	94OE 67A opx11	94OE 67A spl24	94OE 67C cpx8	94OE 67C ol25	94OE 67C mg1	94OE 67C opx1	94OE 67C ol2	94OE 67C cpx14	94OE 67C spl3
SiO ₂	47.76	65.21	43.65	36.52	0.04	41.21	40.98	55.62	0.05	50.74	39.70	0.10	56.23	41.42	53.62	0.07
TiO ₂	2.20	0.04	0.06	5.87	15.94	0.00	0.00	0.03	0.08	1.63	0.06	17.75	0.00	0.00	0.04	0.06
Cr ₂ O ₃	0.17	0.00	0.00	0.02	0.04	0.05	0.06	0.41	17.77	0.03	0.00	0.70	0.45	0.02	0.61	20.15
Al ₂ O ₃	6.42	19.62	33.84	14.18	3.60	0.02	0.00	3.82	50.13	3.18	0.04	1.36	3.20	0.01	3.38	49.12
Fe ₂ O ₃ ^a	2.37	0.24	0.00	8.71	33.94	0.00	0.00	0.10	2.85	2.05	0.00	33.59	0.00	0.00	0.76	2.75
FeO	3.55	0.00	0.47	8.25	43.14	8.46	10.39	6.65	10.42	4.55	18.44	40.41	6.20	9.55	1.66	8.78
MnO	0.12	0.02	0.03	0.22	0.85	0.08	0.17	0.19	0.00	0.13	0.36	0.90	0.18	0.12	0.15	0.00
MgO	13.57	0.00	0.04	13.30	1.46	50.57	48.99	32.80	19.52	14.18	43.09	3.90	33.67	49.70	17.10	20.62
CaO	23.72	0.83	1.96	0.14	0.00	0.05	0.11	0.69	0.04	23.54	0.25	0.14	0.61	0.03	22.93	0.07
Na ₂ O	0.41	4.47	15.57	0.48	0.00	0.01	0.03	0.08	0.00	0.60	0.01	0.01	0.01	0.00	0.61	0.00
K ₂ O	0.01	10.06	4.99	9.11	0.00	0.02	0.00	0.01	0.00	0.05	0.00	0.02	0.00	0.01	0.00	0.01
H ₂ O ^a				4.09												
Total	100.29	100.49	100.62	100.89	99.01	100.48	100.73	100.39	100.87	100.67	101.95	98.88	100.55	100.87	100.87	101.63
Si	1.777	2.939	1.067	2.676	0.002	0.998	0.999	1.918	0.001	1.879	0.992	0.004	1.930	1.005	1.930	0.002
Ti	0.062	0.001	0.001	0.324	0.445	0.000	0.000	0.001	0.002	0.046	0.001	0.492	0.000	0.000	0.001	0.001
Cr	0.005	0.000	0.000	0.001	0.001	0.001	0.001	0.011	0.372	0.001	0.000	0.020	0.012	0.000	0.018	0.419
Al	0.282	1.042	0.975	1.224	0.158	0.001	0.000	0.155	1.565	0.139	0.001	0.059	0.129	0.000	0.143	1.521
Fe ³⁺	0.066	0.008	0.000	0.480	0.948	0.000	0.000	0.003	0.057	0.057	0.000	0.931	0.000	0.000	0.021	0.054
Fe ²⁺	0.110	0.000	0.010	0.506	1.339	0.171	0.212	0.192	0.231	0.141	0.386	1.245	0.178	0.194	0.050	0.193
Mn	0.004	0.001	0.001	0.014	0.027	0.002	0.004	0.005	0.000	0.004	0.008	0.028	0.005	0.003	0.005	0.000
Mg	0.753	0.000	0.002	1.452	0.081	1.825	1.780	1.686	0.771	0.783	1.605	0.214	1.722	1.797	0.917	0.808
Ca	0.946	0.040	0.051	0.011	0.000	0.001	0.003	0.026	0.001	0.934	0.007	0.006	0.023	0.001	0.884	0.002
Na	0.029	0.390	0.738	0.069	0.000	0.001	0.002	0.005	0.000	0.043	0.001	0.001	0.001	0.000	0.042	0.000
K	0.000	0.579	0.156	0.852	0.000	0.001	0.000	0.000	0.000	0.003	0.000	0.001	0.000	0.000	0.000	0.000
OH ^a				2.000												
X _{Mg} (Fe ²⁺)	0.872			0.742		0.912	0.890	0.898		0.847	0.798		0.906	0.901	0.948	
X _{Mg} (Fe ³⁺)	0.810			0.596				0.897		0.798			0.906		0.928	
Ab																
An																
Or																

^aCalculated value; mag, magmatic; xen, xenolithic.

et al. [1991] is also very similar and representative analyses are listed in Table 3.

[13] The peridotite xenoliths consist of olivine (Fo₉₀₋₉₂), enstatite (En₈₉Fs₀₉Wo₀₂) with 3.1–3.3 wt% Al₂O₃, diopside (Di₄₅En₂₆Wo₂₉) with 3–6 wt% Al₂O₃, and brownish-red transparent Cr-spinel with ~60 mol% spinel, 20% hercynite, and 15–16% magnesiochromite (Tables 2 and 3). At the xenolith rims melt infiltrated along olivine rims which produced opaque ulvöspinel with ca. 20 mol% magnesioferrite and 25% magnetite components. This ulvöspinel is surrounded by tiny newly grown olivine grains.

5. Discussion

[14] Immiscibility in alkaline magmas was, for example, discussed by *Philpotts* [1976]. The leucocratic (phonolitic) melt droplets observed in mafic alkaline magma at Jebel Fayah and at Rusayl suggest immiscibility. The whole rock chemistry of the primary basaltic magma and estimates for the leucocratic magma based on the analyzed mineral compositions suggest that the observed compositions probably plot on the two sides of a two-liquid field [*Roedder*, 1951; *Philpotts*, 1982]. Whereas at Jebel Fayah liquid immiscibility seems to be frozen in an early stage (small and mainly round leucocratic droplets), droplets seem to have coalesced at Rusayl to form 5 cm large irregular patches.

[15] The alkaline volcanic rocks of the Qahlah Formation are Maastrichtian-Paleocene in age [*Glennie et al.*, 1974; *Wyns et al.*, 1992a]. The alkali olivine basalts of the Haushi-Huqf area [*Oterdoom et al.*, 1999] may belong to the same volcanism, because they occur in vicinity of the same fault zone, or they may be related to the younger Eocene stage. The pillow lavas of the Al Askharah region may also belong to the early or the Eocene alkaline magmatism. The location of these volcanic rocks points to an association with the horst and graben tectonics which lifted the Haushi-Huqf and the Jebel Ja'alan areas up relative to the surrounding terrain [*Filbrandt et al.*, 1991; *Würsten et al.*, 1991; *Wyns et al.*, 1992a]. This movements also caused syndimentary deforma-

tion which again is dated as Maastrichtian to Paleocene [*Filbrandt et al.*, 1991; *Wyns et al.*, 1992a]. The horst and graben development is put in relation with the oblique thrusting of the Eastern Ophiolite Belt-Batain nappe system onto the eastern edge of the Arabian continent [e.g., *Gnos et al.*, 1997]. Although Jebel Ja'alan is situated in a forebulge position with respect to the Eastern Ophiolite Belt-Batain nappe thrust system, it is unlikely that the loading from this relatively thin nappe stack (<10 km) alone would be sufficient unless thrusting along reactivated faults occurred. The early thrusting (obduction) of the Semail ophiolite was similarly associated with alkaline volcanism [*Allemann and Peters*, 1972; *Robertson et al.*, 1990; *Hacker et al.*, 1996] which suggests that loading of a continental edge with an ophiolite causes deep-reaching deformation in the continental crust manifested by localized alkaline magmatism due to extension.

[16] The mantle xenolith-bearing alkaline lavas found in the Batain and Haushi-Huqf areas, and in the Central Oman Mountains crosscut Paleocene and older strata. They were dated in the Batain region at 37 ± 1 to 44 ± 1 (whole rock K-Ar method) (*Ries et al.*, unpublished report, 1985). This second, Eocene stage of alkaline magmatism is observed in the Batain area, it is possibly present in the Haushi-Huqf area, and it is found near Muscat. Basaltic intrusions of this type, however, are not observed in the crystalline basement nor the sedimentary rocks in southern Oman. This relatively restricted occurrence, the fact that the alkaline magmatism is clearly older than the initiation of the Red Sea (Afar) rifting [*Courtillot et al.*, 1999], and the absence of regional extensional tectonic in the Eocene sedimentary strata [e.g., *Carbon*, 1996] indicate that the Eocene alkaline magmatism is related with local plate reorganization in the Gulf of Oman. In Late Eocene the subduction zone located on the eastern side of the Gulf of Oman that led to ophiolite obduction in southern Pakistan choked [*Gnos et al.*, 1998]. This probably caused reorganization of the plates in the Gulf of Oman region followed by rifting in the Owens Basin [*Mountain and Prell*, 1990], and reactivation of fault systems in the adjacent

Arabian continental margin along which the alkaline melts intruded.

[17] The presence of spinel-bearing mantle xenoliths in the Oman case indicates that brittle deformation reached upper mantle levels (ca. 50 km) and the Al-content of xenolith orthopyroxene suggests upper mantle equilibrium temperatures of $\sim 950^{\circ}\text{C}$.

Acknowledgments

[18] Hilal Al-Azri, Director General of Mineral Resources, Ministry of Commerce and Industry, Sultanate of Oman is thanked for providing logistic help. Ruth Mäder provided FeO and H_2O^+ determinations. EMP work was made possible by the Swiss National Fonds grant 21-26579.89. J. W. Shervais and two anonymous persons are thanked for their reviews.

References

- Al-Harthy, M. S., R. G. Coleman, M. W. Hughes-Clarke, and S. S. Hanna, Tertiary basaltic intrusions in the Central Oman Mountains, in *Ophiolite Genesis and the Evolution of Oceanic Lithosphere*, edited by T. Peters, A. Nicolas, and R. G. Coleman, pp. 675–682, Kluwer Acad., Norwell, Mass., 1991.
- Allemann, F., and T. Peters, The ophiolite-radiolarite belt of the North-Oman Mountains, *Eclogae Geol. Helv.*, **65**, 657–697, 1972.
- Béchenneq, F., J. Roger, S. Chevrel, and J. Le Métour, Explanatory notes to geological map of Al Ashkharah, Sheet NF 40-12, scale 1:250'000, Oman Minist. of Petrol. and Miner., Muscat, 1992.
- Carbon, D., Tectonique post-obduction des montagnes d'Oman dans le cadre de la convergence Arabie-Iran, Ph.D. Thesis, Univ. Montpellier II, Montpellier, 1996.
- Courtillot, V., C. Jaupart, I. Manighetti, P. Tapponnier, and J. Besse, On causal links between flood basalts and continental breakup, *Earth Planet. Sci. Lett.*, **166**, 177–195, 1999.
- Dubreuilh, J. F., A. Béchenneq, J. Berthiaux, J. P. Le Métour, J. Platel, J. Roger, and R. Wyns, Geological map of Khaluf, sheet NF 40-15, scale 1:250'000, Sultanate of Oman, Minist. of Petrol. and Miner., Muscat, 1992a.
- Dubreuilh, J., J. P. Platel, J. Le Métour, J. Roger, R. Wyns, F. Béchenneq, and A. Berthiaux, Explanatory notes, Geological map of Khaluf, sheet NF 40-15, scale 1:250'000, Oman Minist. of Petrol. and Miner., Muscat, 1992b.
- Filbrandt, J. B., S. C. Nolan, and A. C. Ries, Late Cretaceous and early Tertiary evolution of Jebel Ja'alan and adjacent areas, NE Oman, in *Geology and Tectonics of the Oman Region*, edited by A. H. F. Robertson, M. P. Searle, and A. C. Ries, Geol. Soc. Spec. Publ., **49**, 697–714, 1991.
- Glazner, A. F., and J. M. Bartley, Eruption of alkali basalts during crustal shortening in southern California, *Tectonics*, **13**, 493–498, 1994.
- Glennie, K. W., M. G. A. Boeuf, M. W. Hughes-Clark, M. Moody-Stuart, W. F. H. Pilar, and B. M. Reinhardt, *Geology of the Oman Mountains*, vol. 31, 423 pp., Verhandelingen van het Koninklijk Nederlands Geol. Mijnbouwkundig Genootschap, 1974.
- Gnos, E., and M. Perrin, Formation and evolution of the Masirah ophiolite constrained by paleomagnetic study of volcanic rocks, *Tectonophysics*, **253**, 53–64, 1995.
- Gnos, E., A. Immenhauser, and T. Peters, Late Cretaceous/Early Tertiary convergence between the Indian and Arabian plates recorded in ophiolites and related sediments, *Tectonophysics*, **271**, 1–19, 1997.
- Gnos, E., M. Khan, K. Mahmood, A. S. Khan, N. A. Shafique, and I. M. Villa, Bela oceanic lithosphere assemblage and its relation to the Réunion hotspot, *Terra Nova*, **10**, 90–95, 1998.
- Hacker, B., J. Mosenfelder, and E. Gnos, Rapid emplacement of the Oman ophiolite: Thermal and geochronological considerations, *Tectonics*, **15**, 1230–1247, 1996.
- Hauser, M., The allochthonous sedimentary and volcanic rock record from the Batain plain (Sultanate of Oman), Ph.D. thesis, Bern Univ., Bern, Switzerland, 2000.
- Immenhauser, A., G. Schreurs, T. Peters, A. Matter, M. Hauser, and P. Dumitrica, Stratigraphy, sedimentology and depositional environments of the Permian to uppermost Cretaceous Batain Group, eastern-Oman, *Eclogae Geol. Helv.*, **91**, 217–235, 1998.
- Immenhauser, A., G. Schreurs, E. Gnos, H. W. Oterdoom, and B. Hartmann, Late Palaeozoic to Neogene geodynamic evolution of the northeastern Oman margin, *Geol. Magazine*, **137**, 1–18, 2000.
- Le Maitre, R. W., et al., Classification of igneous rocks and glossary of terms, Blackwell Sci., Malden, Mass., 1989.
- Le Métour, J. F., F. Béchenneq, J. Roger, and S. Chevrel, Geological map of Al Ashkharah, sheet NF 40-12, scale 1:250'000, with explanatory notes, Sultanate of Oman, Minist. of Petrol. and Miner., Muscat, 1992.
- Morimoto, N., J. Fabries, A. K. Ferguson, I. V. Ginzburg, M. Ross, F. A. Seifert, J. Zussman, K. Aoki, and G. Gottardi, Nomenclature of pyroxenes, *Schweizerische Mineralogische und Petrographische Mitteilungen*, **68**, 95–111, 1988.
- Moser, L., The Ruwaydah Unit; Volcanic and limestone deposits of a dismembered seamount, MS thesis, Bern Univ., Bern, Switzerland, 2000.
- Mountain, G. S., and W. L. Prell, A multiphase plate tectonic history of the southeast continental margin of Oman, in *The Geology and Tectonics of the Oman Region*, edited by A. H. F. Robertson, M. P. Searle, and A. C. Ries, Geol. Soc. Spec. Publ., **49**, 725–744, 1990.
- Oterdoom, H., M. A. Worthing, and M. Partington, Petrological and tectonostratigraphic evidence for a mid Ordovician rift pulse on the Arabian Peninsula, *Geoarabia*, **4**, 467–500, 1999.
- Peters, T., M. Al-Batashy, H. Bläsi, M. Hauser, A. Immenhasuer, L. Moser, and A. Al Rajhi, Geological map of Sur and Al Ashkharah, sheet NF 40-8F and sheet 40-12C, scale 1:100'000, with explanatory notes, Directorate General of Minerals, Minist. of Comm. and Ind., Muscat, Oman, 2001.



- Philpotts, A. R., Silicate liquid immiscibility: Its probable extent and petrologic significance, *Am. J. Sci.*, 276, 1147–1177, 1976.
- Philpotts, A. R., Compositions of immiscible liquids in volcanic rocks, *Contrib. Mineral. Petrol.*, 80, 201–218, 1982.
- Robertson, A. H. F., C. D. Blome, D. W. J. Cooper, A. E. S. Kemp, and M. P. Searle, Evolution of the Arabian continental margin in the Dibba Zone, Northern Oman Mountains, in *The Geology and Tectonics of the Oman Region*, edited by A. H. F. Robertson, M. P. Searle, and A. C. Ries, *Geol. Soc. Spec. Publ.*, 49, 251–258, 1990.
- Roedder, E., Low temperature liquid immiscibility in the system K_2O - FeO - Al_2O_3 - SiO_2 , *Am. Mineral.*, 36, 282–286, 1951.
- Schreurs, G., and A. Immenhauser, West-northwest directed obduction of the Batain Group on the eastern Oman continental margin at the Cretaceous-Tertiary boundary, *Tectonics*, 18, 148–160, 1999.
- Shackleton, R. M., et al., The Batain Melange of NE Oman, in *Geology and Tectonics of the Oman Region*, edited by A. H. F. Robertson, M. P. Searle, and A. C. Ries, *Geol. Soc. Spec. Publ.*, 49, 673–696, 1990.
- Würsten, F., M. Flisch, I. Michalski, J. Le Métour, I. Mercolli, U. Matthäus, and T. Peters, The uplift history of the Precambrian crystalline basement of the Jabal J'alan (Sur area), in *Ophiolite Genesis and the Evolution of Oceanic Lithosphere*, edited by T. Peters, A. Nicolas, and R. G. Coleman, pp. 613–626, Kluwer Acad., Norwell, Mass., 1991.
- Wyns, R., F. Béchenec, J. Le Métour, J. Roger, and S. Chevrel, Explanatory notes, Geological map of Sur, sheet NF 40-08, scale 1:250'000, Sultanate of Oman, Minist. of Petrol. and Miner., Muscat, 1–103, 1992a.
- Wyns, R., F. Béchenec, J. Le Métour, J. Roger, and S. Chevrel, Geological map of Sur, sheet NF 40-08, scale 1:250'000, with explanatory notes, Directorate General of Minerals, Oman Minist. of Petrol. and Miner., Muscat, 1992b.